

acetonitrile was removed in vacuo. Drying the isolated material [25 °C (0.5 mmHg)] produced an orange-yellow solid. Chromatography on a column of silica gel (chloroform elution) provided 10 g (53%) of a yellow solid. Crystallization of 4 from ethanol provided 7.7 g (40%) of fluffy, light yellow crystals: mp 171.5–172.5 °C; IR (KBr) 3080, 3020 (Ar, C–H), 2960 (Et, C–H), 2916, 2860 (Et, C–H), 1690 (C=O), 1610, 1520 (NO₂), 1450, 1350 (NO₂), 1270, 850, 820, 730, 695 cm⁻¹; ¹H NMR (CDCl₃–1% Me₄Si) δ 2.47 (s, 3 H, COCH₃), 6.76–8.14 (m, 16 H, ArH). Anal. Calcd for C₂₇H₁₉NO₃: C, 79.98; H, 4.72; N, 3.46. Found: C, 79.69; H, 4.76; N, 3.39.

9-(4-Nitrophenyl)-9-[4'-(2-methyl-1,3-dioxolan-2-yl)-phenyl]fluorene (5). A liquid–liquid suspension of 2.0 g (4.9 mmol) of 4, 0.86 mL (1.5 mmol) of ethylene glycol, 0.035 g (0.56 mmol) of *p*-toluenesulfonic acid monohydrate, and 40 mL of benzene was heated at reflux for 22 h, and approximately 15 mL of the benzene–water azeotrope was siphoned from the Dean–Stark trap. Following 16 h of additional reflux, 15 mL of the benzene–water azeotrope was again removed. Reflux was continued for 53 h and the mixture was cooled to ambient temperature. The reaction mixture was diluted with 80 mL of benzene, and washed with 10% sodium hydroxide (3 × 5 mL) and 5% sodium bicarbonate (2 × 10 mL). The benzene layer was dried with magnesium sulfate, and the solvent was removed to give 1.9 g (86%) of yellow solid 5. Crystallization of 5 from a benzene–hexane solvent mixture gave, after drying [105 °C (0.5 mmHg)], 1.6 g (73%) of fluffy light green 5: mp 215–216 °C; IR (KBr) 3040 (Ar, C–H), 3000, 2950, 2890 (CH₂), 1610, 1525 (NO₂), 1455, 1350 (NO₂), 1200, 1040, 830, 750, 700 cm⁻¹; ¹H NMR (CDCl₃–1% Me₄Si) δ 1.57 (s, 3 H, CH₃), 3.82 (A₂B₂, m, 4 H, CH₂), 6.82–8.10 (m, 16 H, ArH). Anal. Calcd for C₂₉H₂₃NO₄: C, 77.49; H, 5.16; N, 3.12. Found: C, 77.20; H, 5.01; N, 2.85.

9-[5-(3-Phenyl-2,1-benzisoxazolyl)]-9-[4'-(2-methyl-1,3-dioxolan-2-yl)phenyl]fluorene (6). A mixture of 0.88 g (22 mmol) of sodium hydroxide, 5 mL of methanol, and 15 mL of tetrahydrofuran was stirred for 15 min. This mixture was cooled (ice), and 0.49 mL (0.5 g, 4.2 mmol) of phenylacetonitrile was added. After 15 min of stirring, 1.27 g (2.83 mmol) of 5 and 1.0 mL of tetrahydrofuran were added. The dark green reaction mixture was stirred and cooled (ice) for 30 min and then heated at reflux for 16 h. While the mixture was still warm, 100 mL of methanol was added, followed by cooling of the heterogeneous mixture to ambient temperature. Filtering the suspended solid provided a beige powder that, when washed with 500 mL of methanol (or until the washings turned colorless), air-dried (aspirator), and dried under reduced pressure [25 °C (0.5 mmHg)], afforded 1.3 g (89%) of light beige powder 6. This material was crystallized from a benzene–hexane mixture, affording 1.0 g (69%) of fluffy, light beige crystalline 6 after drying [105 °C (0.5 mmHg)]: mp 247–248 °C; IR (KBr) 3170 (Ar, C–H), 2990, 2890 (CH₂), 1645 (C=N), 1560, 1525, 1500, 1475, 1445, 1370, 1250, 1040, 800, 740, 680 cm⁻¹; ¹H NMR (CDCl₃–1% Me₄Si) δ 1.58 (s, 3 H, CH₃), 3.82 (A₂B₂, m, 4 H, CH₂), 6.89–7.87 (m, 20 H, ArH). Anal. Calcd for C₃₆H₂₇NO₃: C, 82.90; H, 5.22; N, 2.69. Found: C, 82.94; H, 5.42; N, 2.79.

9-(4-Amino-3-benzoylphenyl)-9-[4'-(2-methyl-1,3-dioxolan-2-yl)phenyl]fluorene (7). A suspension of 0.80 g (1.5 mmol) of 6, 0.061 g of 5% palladium-on-charcoal, 6.5 mL of tetrahydrofuran, and 0.21 mL of triethylamine was subjected to a hydrogen atmosphere, at ambient temperature, until gas uptake ceased. Filtration of the resulting mixture, followed by removal of the solvent from the filtrate, provided 0.79 g (98%) of a yellow solid. This solid was crystallized from a benzene–hexane solvent mixture, providing, after drying [105 °C (0.5 mmHg)], 0.58 g (72%) of 7 as yellow crystals: mp 165.0–166.5 °C; IR (KBr) 3480 (NH₂), 3350 (NH₂), 3060 (Ar, C–H), 2990, 2890 (CH₂), 1625 (C=O), 1580, 1545, 1445, 1245, 1030, 815, 740, 700, 645 cm⁻¹; ¹H NMR (CDCl₃–1% Me₄Si) δ 1.55 (s, 3 H, COCH₃), 3.78 (A₂B₂, m, 4 H, CH₂), 5.83 (s, br, 2 H, ArNH₂), 6.28–7.72 (m, 20 H, ArH). Anal. Calcd for C₃₆H₂₉NO₃: C, 82.58; H, 5.58; N, 2.68. Found: C, 81.83; H, 5.59; N, 2.58.

9-(4-Amino-3-benzoylphenyl)-9-(4'-acetylphenyl)fluorene (8). To a solution of 1.8 g (3.4 mmol) of 7 in 12 mL of tetrahydrofuran was added 12 mL of 0.6 N hydrochloric acid, and the mixture was stirred at 25 °C for 24 h. Dilution of the reaction mixture with 12 mL of water, followed by removal of the tetra-

hydrofuran in vacuo, produced a suspension of yellow solid in water. The solid was removed by filtration and washed with water until the washings were neutral (pH paper). The precipitate was then dissolved in chloroform, washed with a 10% sodium bicarbonate solution and water, and dried over sodium sulfate. Removal of the chloroform in vacuo provided 1.5 g (91%) of a green-yellow solid. Chromatography of this solid on a column of silica gel (dichloromethane elution) and recrystallizations from benzene–methanol, followed by drying [105 °C (0.5 mmHg)], gave 1.3 g (79%) of yellow crystalline 8: mp 205.5–206.5 °C; IR (KBr) 3480 (NH₂), 3350 (NH₂), 3060 (Ar, C–H), 2930 (Me, C–H), 1680 (C=O), 1600, 1550, 1450, 1265, 1250, 1170, 820, 735, 700, 650 cm⁻¹; ¹H NMR (CDCl₃–1% Me₄Si) δ 2.40 (s, 3 H, COCH₃), 5.90 (s, br, 2 H, ArNH₂), 6.25–7.81 (m, 20 H, ArH); ¹³C NMR (CDCl₃–1% Me₄Si) δ 198.2 (C=O), 197.3 (C=O), 151.1, 150.3, 149.6, 139.8, 139.2, 135.4, 133.8, 133.6, 131.5, 129.1, 128.2, 127.6, 125.6, 120.2, 117.5, 117.1, 64.4, 26.6. Anal. Calcd for C₃₄H₂₅NO₂: C, 85.15; H, 5.25; N, 2.92. Found: C, 85.36; H, 5.09; N, 2.89.

Polymerization. Poly[2-(*p*-phenylene)-4-phenyl-6-[9-(*p*-phenylene)-9'-fluorenylidene]quinoline] (9) was prepared by using polymerization conditions similar to those for the AA–BB polyquinolines.² A mixture of 1.000 g (2.085 mmol) of 9-(4-amino-3-benzoylphenyl)-9-(4'-acetylphenyl)fluorene (8), 15 g (50 mmol) of di-*m*-cresyl phosphate, and 4.8 mL of *m*-cresol was heated at 135–140 °C under a static nitrogen atmosphere, with mechanical stirring, for 46 h. Precipitation of this amber-colored reaction mixture into 350 mL of a 10% triethylamine–90% ethanol mixture afforded fibrous material. Collection of the polymer by suction filtration and extraction in an amine–ethanol mixture for 48 h afforded 0.918 g (99.3%) of small, beige fiber strands. Anal. Calcd for (C₃₉H₂₁N₇)_n: C, 92.07; H, 4.77; N, 3.16. Found: C, 91.00; H, 5.01; N, 3.43, residue 0.57.

Solution viscosities were measured in *m*-cresol with a Cannon–Ubbelohde microdilution viscometer at 25.0 ± 0.1 °C. The intrinsic viscosity, [η] = 0.24 dL/g, was obtained from extrapolation of reduced and inherent viscosities to zero concentration.

Thermal analyses were conducted with a Du Pont 990 differential thermal analyzer equipped with a differential scanning calorimeter (DSC) cell base module II and a 950 thermogravimetric analyzer (TGA). The DSC analysis was obtained on pressed powder samples at a heating rate of 10 °C/min under a nitrogen flow of 50–60 mL/min. Thermogravimetric analysis was carried out on slightly pressed, powdered polyquinolines at a 5 °C/min heating rate in both flowing air and nitrogen atmospheres (flow rate 50–60 mL/min).

Acknowledgment. This research was supported by the U.S. Army Research Office, Research Triangle, N.C.

References and Notes

- (1) Korshak, V. V.; Vinogradova, S. V.; Vygodski, Y. S. *J. Macromol. Sci., Rev. Macromol. Chem.* **1974**, *44*, 1613.
- (2) Stille, J. K.; Harris, R. M.; Padaki, S. M. *Macromolecules* **1981**, *14*, 486.
- (3) (a) Eaborn, C.; Golesworthy, R. C.; Lilly, M. N. *J. Chem. Soc.* **1961**, 3052. (b) Bolton, R.; Chapman, N. B.; Shorter, J. *Ibid.* **1964**, 1895.
- (4) Adams, R.; Campbell, J. *J. Am. Chem. Soc.* **1950**, *72*, 153.
- (5) Nunno, L. D.; Florio, S.; Todesco, P. E. *J. Chem. Soc. C* **1970**, 1433.
- (6) Daniher, F. A. *Org. Prep. Proced.* **1970**, *2*, 207.
- (7) David, R. B.; Pizzini, L. C. *J. Org. Chem.* **1960**, *25*, 1884.
- (8) Norris, S. O.; Stille, J. K. *Macromolecules* **1976**, *9*, 496.

Does a Glassy Polymer on Annealing Relax toward the Equilibrium State?

RYONG-JOON ROE

Department of Materials Science and Metallurgical Engineering, University of Cincinnati, Cincinnati, Ohio 45221. Received March 16, 1981

When a glassy polymer is brought to a temperature moderately below its *T_g*, it undergoes a slow relaxation toward a limiting structural state. Such relaxation is

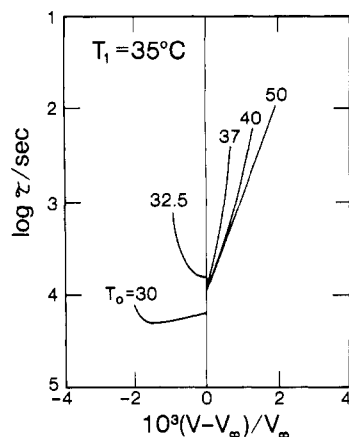


Figure 1. Schematic illustration of the data by Kovacs⁷ on volume relaxation of poly(vinyl acetate). The effective relaxation time τ is plotted against the deviation from "equilibrium". Samples, at first brought to virtual equilibrium at temperature T_0 , were allowed to undergo relaxation at temperature T_1 .

manifested by changes with time in such observable properties as volume, enthalpy, mechanical moduli, etc. The limiting state toward which the relaxation proceeds is usually considered to correspond to the equilibrium state coinciding with the liquid structure extrapolated through T_g down to the temperature of interest.

There are, however, two types of observations which seem to suggest that the limiting state might not be an equilibrium state. The first of these relates to the thermal density fluctuation observable with small-angle X-ray scattering. For liquids or amorphous polymers the scattered intensity, extrapolated to zero scattering angle, is given¹ by

$$I(0) = \rho k T \kappa_T \quad (1)$$

where ρ is the electron density and κ_T the isothermal compressibility. It has been shown²⁻⁴ for a number of polymers that eq 1 is well obeyed above T_g , while below T_g the observed $I(0)$ is consistently higher than predicted by eq 1. Recently Wendorff⁵ reported that a polycarbonate sample was annealed at 125 °C for up to 1000 h, but the observed $I(0)$ remained at the same initial value, which was much higher than given by eq 1. A similar result was also obtained in our laboratory.⁶ The full implication of these observations is not clear at present. It could mean that the state to which a glassy polymer relaxes on annealing indeed differs from the equilibrium liquid. It could also mean simply that the relaxation time for the property revealed by $I(0)$ is longer, by several orders of magnitude, than the relaxation times of volume and enthalpy.

The second type of observation suggesting a nonequilibrium nature of the limiting annealed state was reported in the early work by Kovacs⁷ on volume relaxation of poly(vinyl acetate). The salient feature of his result is shown schematically in Figure 1. From the change in volume, observed isothermally at 35 °C with dilatometry, the effective relaxation time was calculated according to

$$d\Delta v/dt = -(1/\tau)\Delta v \quad (2)$$

where $\Delta v = v_t - v_\infty$, v_∞ being the limiting value of v at long annealing time. Here each curve represents an experimental run in which the sample was initially conditioned until an apparent equilibrium volume corresponding to the

temperature T_0 is reached, and thereafter it was quickly transferred to the common annealing temperature T_1 and the change in volume with time followed. The original work of Kovacs⁷ shows results obtained at various combination of T_0 and T_1 , but here only the data for $T_1 = 35$ °C are illustrated. The particular feature to be noted is that when T_0 is higher than T_1 (Δv thus approaching 0 from above), all the curves converge, while they fail to converge when T_0 is smaller than T_1 (and Δv approaches 0 from below).

A number⁸⁻¹⁶ of molecular or phenomenological models have been proposed to explain the kinetics of volume relaxation. Many of them attained degrees of success in reproducing the features depicted in Figure 1 concerning the dependence of τ on Δv as long as T_0 was higher than T_1 . But none of them were able to explain the nonconvergence of the curves which occurs when T_0 is smaller than T_1 . This led Kovacs et al.¹³ to suggest that the assumption, underlying all these theories, of the limiting equilibrium state not depending on previous thermal history might be invalid. If paraphrased, this might mean that the limiting state to which the annealed glass apparently approaches is not a true equilibrium state. It will be shown below, however, that the features depicted in Figure 1 do not necessarily contradict the view that the equilibrium state is eventually reached on long isothermal relaxation.

A macroscopic property, such as volume, of a material in a nonequilibrium state can be represented as a function of T , p , and a set of internal state variables¹⁷ (or order parameters).^{18,19} The internal variables z_i ($i = 1 \dots n$) are functions of T and p in the equilibrium state but can be varied independently in nonequilibrium states. If we write

$$v = v(T, p, \mathbf{z}) \quad (3)$$

where \mathbf{z} is a vector consisting of components z_i ($i = 1 \dots n$), Taylor expansion of v around its equilibrium value leads to

$$\Delta v = \frac{\partial v}{\partial \mathbf{z}} \Delta \mathbf{z} + \dots \quad (4)$$

where Δ represents deviation from the respective equilibrium value. The time derivation of (4) gives

$$\frac{d\Delta v}{dt} = \frac{\partial v}{\partial \mathbf{z}} \frac{d\Delta \mathbf{z}}{dt} + \dots \quad (5)$$

The dynamics of the change in the internal variables \mathbf{z} near their equilibrium point can be written¹⁷ as

$$d\Delta \mathbf{z}/dt = -\mathbf{M}\Delta \mathbf{z} \quad (6)$$

where \mathbf{M} is an $n \times n$ matrix, its element M_{ij} representing the rates of relaxation toward equilibrium. \mathbf{M} is symmetric by virtue of the Onsager reciprocity relation. \mathbf{M} is in general a function of \mathbf{z} under given T and p , but in the vicinity of the equilibrium state, a linear approximation, regarding \mathbf{M} as independent of \mathbf{z} , is valid. By combining eq 2, 4, 5, and 6, we can write¹⁹

$$\tau = \frac{\partial v}{\partial \mathbf{z}} \Delta \mathbf{z} / \left(\frac{\partial v}{\partial \mathbf{z}} \mathbf{M} \Delta \mathbf{z} \right) \quad (7)$$

Approach of the system toward equilibrium is equivalent to $|\Delta \mathbf{z}| \rightarrow 0$. In this limit eq 7 does not converge to a unique value. This can be seen easily by dividing the numerator and denominator of (7) with $|\Delta \mathbf{z}|$. Then the

components of $\Delta z/|\Delta z|$ remain finite as $|\Delta z| \rightarrow 0$ and τ can be evaluated. The value of τ thus obtained depends on the relative magnitudes of the components z_i . If we consider an n -dimensional "configuration" space, in which each coordinate axis represents z_i , then any nonequilibrium state of the system (under constant T and p) can be represented by a point in this configuration space. Equation 6 describes the motion of such a representative point in it. Given sufficient time, trajectories of all representative points will eventually converge to a single point corresponding to the equilibrium state. The same material system having different thermal histories will initially be placed at different regions of the configuration space, and the trajectories, as they approach the equilibrium point, will be different from each other. Consequently, the values of τ given by eq 7 will also be different from each other.

The above discussion shows that the main point depicted in Figure 1, i.e., the limiting τ values of volume relaxation to depend on previous thermal history, can be explained without assuming that the state reached after prolonged annealing is something different from a true equilibrium state. It is also conceivable that volume is a very insensitive indicator of attainment of equilibrium. If that is the case, then even when volume has apparently reached its limit, the structure may still be far from true equilibrium and continues to undergo slow relaxation. As evidence supporting this, we can cite the observation²⁰ that the shape of the endothermic peak of annealed polystyrene, obtained by differential scanning calorimetry, continues to change long after the volume relaxation has achieved apparent completion.

Acknowledgment. A helpful criticism, on an earlier manuscript of this work, by Dr. J. J. Aklonis is gratefully acknowledged. This work was supported in part by the National Science Foundation under Grants DMR77-20876 and DMR80-04236.

References and Notes

- Guinier, A. "X-ray Diffraction"; W. H. Freeman: San Francisco, 1963; p 46. Guinier, A.; Fournet, G. "Small-Angle Scattering of X-rays"; Wiley: New York, 1955; p 71.
- Wendorff, J. H.; Fischer, E. W. *Kolloid Z. Z. Polym.* **1973**, *251*, 876.
- Rathje, J.; Ruland, W. *Colloid Polym. Sci.* **1976**, *254*, 358.
- See Matyi et al. (Matyi, R. J.; Uhlmann, D. R.; Koutsky, J. A. *J. Polym. Sci., Polym. Phys. Ed.* **1980**, *18*, 1053) for the reference to the series of papers on this subject by Uhlmann and co-workers.
- Wendorff, J. H. *J. Polym. Sci., Polym. Lett. Ed.* **1979**, *17*, 765.
- Curro, J. J.; Roe, R. J., unpublished work.
- Kovacs, A. J. *J. Polym. Sci.* **1958**, *30*, 131.
- A. J. Kovacs, *Fortschr. Hochpolym. Forsch.* **1963**, *3*, 394.
- Adam, G. *Kolloid Z. Z. Polym.* **1962**, *180*, 11.
- Bueche, F. *J. Chem. Phys.* **1962**, *36*, 2940.
- Hozumi, S. *Polym. J.* **1971**, *2*, 756.
- Narayanawamy, O. S. *J. Am. Ceram. Soc.* **1971**, *54*, 491.
- Kovacs, A. J.; Hutchinson, J. M.; Aklonis, J. J. In "Proceedings of the Symposium on the Structure of Non-crystalline Materials"; Cambridge University Press: New York, 1976; p 153.
- Debolt, M. A.; Easteal, A. J.; Macedo, P. B.; Moynihan, C. T. *J. Am. Ceram. Soc.* **1976**, *59*, 16.
- Kovacs, A. J.; Aklonis, J. J.; Hutchinson, J. M.; Ramos, A. R. *J. Polym. Sci., Polym. Phys. Ed.* **1979**, *17*, 1097.
- Robertson, R. E. *J. Polym. Sci., Polym. Symp.* **1978**, *63*, 173.
- J. Polym. Sci., Polym. Phys. Ed.* **1979**, *17*, 597.
- de Groot, S. R.; Mazur, P. "Non-Equilibrium Thermodynamics"; North-Holland Publishing Co.: Amsterdam, 1962; p 221.
- Davies, R. O.; Jones, G. O. *Adv. Phys.* **1953**, *2*, 370.
- Roe, R. J. *J. Appl. Phys.* **1977**, *48*, 4085.
- Curro, J. J.; Roe, R. J. *Bull. Am. Phys. Soc.* **1980**, *25*, 283.
- Curro, J. J. M.S. Thesis, University of Cincinnati, 1979.

Static Scattering Function for a Polymer Chain in a Good Solvent

TAKAO OHTA,^{1A,C} YOSHITSUGU OONO,^{1B,C} and KARL F. FREED^{*1B}

Department of Physics, University of Pittsburgh, Pittsburgh, Pennsylvania 15260, Department of Physics, Kyushu University, Fukuoka 812, Japan, and The James Franck Institute and the Department of Chemistry, The University of Chicago, Chicago, Illinois 60637. Received November 24, 1980

The most directly measurable quantity that is related to the spatial structure of a single polymer chain in a good solvent is the static scattering function $S(\mathbf{k})$, which is given by

$$S(\mathbf{k}) = \sum_{i=1}^N \sum_{j=1}^N \langle \exp[i\mathbf{k} \cdot (\mathbf{c}_i - \mathbf{c}_j)] \rangle \quad (1)$$

where \mathbf{c}_i denotes the position of the i th monomer and $\langle \rangle$ the equilibrium ensemble average. Experimental determinations focus on the ratio $I(\mathbf{k}) = S(\mathbf{k})/S(0)$. Let $x = k^2 \langle S^2 \rangle$, where $\langle S^2 \rangle$ is the mean-square radius of gyration and $k = |\mathbf{k}|$. Then $I(x)$ is a universal function of x . For a Gaussian chain, the ratio $I_0(x)$ is given by

$$I_0(x) = 2 \left(\frac{1}{x} + \frac{e^{-x}}{x^2} - \frac{1}{x^2} \right) \quad (2)$$

Witten and Schäfer² recently used renormalization theory to calculate the leading two nontrivial terms in the series expansion of $I(x)$ in powers of x to order $\epsilon = 4 - d$, where d is the spatial dimension. They note that $I_0(x) > I(x)$ for smaller x . In the $x \rightarrow \infty$ limit these scattering functions behave as $I(x) \sim x^{-1/2\nu}$ ($\nu \sim 3/5$) and $I_0(x) \sim x^{-1}$, but this appears to occur beyond the currently accessible experimental range, i.e., for $x > 100$. In this limit $I(x) > I_0(x)$, and as is noted by Witten and Schäfer,² there must be an x_c such that $I(x_c) = I_0(x_c)$.

We provide a closed-form expression for $I(x)$ to order ϵ for fully developed excluded volume. The result is obtained for all values of x , the limiting $x \rightarrow 0$ and $x \rightarrow \infty$ regions, and the intermediate regime that is inaccessible to scaling theories. Our calculational method is based on the Gell-Mann-Low type renormalization group theory, which is formulated in chain configuration space.³ The theoretical details will be published elsewhere;⁴ here we concentrate on the final results. The closed form of $I(x)$ is given by

$$I(x) = e^{-\epsilon/8} f(\beta) \quad (3)$$

where

$$\beta = dx/3(1 - 13\epsilon/96)$$

and

$$\begin{aligned} f(\beta) = I_0(\beta) \exp[-\epsilon g(\beta)/4I_0(\beta)] \\ g(\beta) = 2 \int_0^1 dt \left[\frac{e^{-\beta}}{\beta^2} A[\beta - \beta t(1-t)] + \left(\frac{1}{\beta} - \frac{1}{\beta^2} \right) A(-\beta t(1-t)) - \frac{1 - \exp[-\beta t(1-t)]}{\beta^2 t(1-t)} \right] + \\ \int_0^1 dt \left[\frac{1}{\beta(1-t)} + \frac{\exp[-\beta t(1-t)] - 1}{\beta^2 t(1-t)^2} \right] - \frac{1}{\beta^2} e^{-\beta} A(\beta) + \frac{1}{\beta} e^{-\beta} A(\beta) + \frac{1}{\beta} e^{-\beta} \\ A(x) = \int_0^x dt (e^t - 1)/t \end{aligned}$$